Biogeosciences Discuss., 10, 11969–12008, 2013
www.biogeosciences-discuss.net/10/11969/2013/
doi:10.5194/bgd-10-11969-2013

Biogeosciences Discussions
Open Access

Nutrient regimes control phytoplankton ecophysiology in the South Atlantic

T. J. Browning[1], H. A. Bouman[1], C. M. Moore[2], C. Schlosser[2], G. A. Tarran[3], E. M. S. Woodward[3], and G. M. Henderson[1]

[1]Department of Earth Sciences, University of Oxford, South Parks Road, Oxford, UK
[2]Ocean and Earth Science, National Oceanography Centre Southampton, University of Southampton, European Way, Southampton, UK
[3]Plymouth Marine Laboratory, Prospect Place, The Hoe, Plymouth, UK

Received: 9 July 2013 – Accepted: 12 July 2013 – Published: 17 July 2013

Correspondence to: T. J. Browning (thomasb@earth.ox.ac.uk)

Published by Copernicus Publications on behalf of the European Geosciences Union.

Abstract

Fast Repetition Rate fluorometry (FRRf) measurements of phytoplankton photophysiology from an across-basin South Atlantic cruise (as part of the GEOTRACES programme) characterized two dominant ecophysiological regimes which were interpreted on the basis of nutrient limitation. South of the South Subtropical Convergence (SSTC) in the northern sub-Antarctic sector of the Antarctic Circumpolar Current (ACC) in the Eastern Atlantic Basin, waters are characterized by elevated chlorophyll concentrations, a dominance by larger phytoplankton cells, and low apparent photochemical efficiency (F_v/F_m). Shipboard 24 h iron (Fe) addition incubation experiments confirmed that Fe stress was primarily responsible for the low F_v/F_m, with Fe addition to these waters, either within the artificial bottle additions or naturally occurring downstream enrichment from Gough Island, significantly increasing F_v/F_m values. Satellite images suggest a broader region of enhanced chlorophyll concentrations around the SSTC in the Western Atlantic relative to the Eastern Atlantic: hypothesized to be a result of higher iron supply from the South American continent. To the north of the SSTC at the southern boundary of the South Atlantic Gyre, phytoplankton are characterized by high values of F_v/F_m which, coupled with the low macronutrient concentrations and increased presence of picocyanobacteria, are interpreted as conditions of Fe replete, balanced macronutrient-limited growth. Spatial correlation was found between F_v/F_m and Fe : nitrate ratios, supporting the suggestion that the relative supply ratios of these two nutrients can control patterns of limitation and consequently the ecophysiology of phytoplankton in subtropical gyre and ACC regimes.

1 Introduction

The chlorophyll concentrations of the world's surface oceans are well constrained through satellite images of ocean colour. However, knowledge of the standing crop of phytoplankton is insufficient to understand the role of ocean primary production on

BGD
10, 11969–12008, 2013

global nutrient and carbon cycles, which will also be strongly influenced by the phytoplankton community structure and physiological status (Katz et al., 2004; Behrenfeld and Falkowski, 1997). In turn, the ecology and physiology of phytoplankton are regulated by multiple driving factors including light, temperature, nutrient availability, and grazing rates (Boyd et al., 2010). Globally, nutrient limitation of phytoplankton standing crops and growth rates has been shown to be dominated by the availability of fixed inorganic nitrogen, primarily in the form of nitrate, and iron (Fe) (Moore et al., 2013). However, the spatial resolution of data describing nutrient limitation is low, with large areas remaining poorly sampled (Moore et al., 2013). Such under-sampling is partly a result of the effort involved in conducting, and difficulties in unambiguously interpreting, shipboard bioassay incubation experiments where the phytoplankton population has been removed from their in situ environment (Cullen et al., 1992; Moore et al., 2013). The physiological assessment of phytoplankton communities using Fast Repetition Rate fluorometry (FRRf) represents a possible means of rapidly diagnosing nutrient limitation of phytoplankton (Greene et al., 1994). However, a variety of factors can influence FRRf derived photophysiological parameters (e.g. the apparent photochemical efficiency, F_v/F_m) under multi-faceted ecophysiological regimes (Behrenfeld et al., 2006; Moore et al., 2006a, 2008; Suggett et al., 2009; Schrader et al., 2011; Behrenfeld and Milligan, 2013). Thus, while many studies have suggested that FRRf signatures are influenced by nutrients, the prevailing light climate and/or the phytoplankton community structure, the factors which dominate the signal under different circumstances remain a subject of debate (Suggett et al., 2009; Behrenfeld and Milligan, 2013).

Although the exact causative mechanisms remain to be fully established (Behrenfeld and Milligan, 2013), Fe additions to Fe-limited waters have been repeatedly shown to increase F_v/F_m (Greene et al., 1994; Kolber et al., 1994; Behrenfeld et al., 1996; Olson, 2000; Boyd and Abraham, 2001; Sosik and Olson, 2002; Moore et al., 2006a, 2007). In contrast, in macronutrient-limited subtropical gyre waters F_v/F_m values have typically been found to be higher than for Fe-limited waters and insensitive to nitrate and/or phosphate additions (Behrenfeld et al., 2006; Moore et al., 2008; see also Parkhill

BGD
10, 11969–12008, 2013

et al. (2001) for analogous laboratory experiments). The reasons for this differential response remain uncertain, although one possibility is that the phytoplankton in these waters are living under conditions of balanced nutrient-limited growth, rather than starvation, as a result of sustained nutrient (re-)supply due to rapid efficient recycling (Moore et al., 2008).

The South Subtropical Convergence (SSTC) is the intersection point of low macronutrient subtropical gyre waters and high macronutrient ACC waters and therefore represents one of the most dynamic nutrient environments in the oceans (Ito et al., 2005). Satellite images show chlorophyll concentrations in the SSTC are typically elevated with respect to subtropical gyre waters further north and Antarctic Circumpolar Current (ACC) waters to the south throughout the year, although peak concentrations are found during austral spring and summer (Longhurst, 1998). Suggested mechanisms explaining the enhanced phytoplankton standing crop of the SSTC principally revolve around the idea that convergence of subtropical gyre waters, generally considered to be limited by the availability of nitrate (e.g. Dugdale and Goering, 1967; Ryther and Dunstan, 1971; Eppley et al., 1979), and ACC waters, generally considered to be limited by Fe availability (e.g. Boyd et al., 2000), provide both nitrate and Fe to the region, thus producing a nutrient regime that is capable of supporting elevated phytoplankton standing crops (Longhurst, 1998; Ito et al., 2005). The stability of the upper water column, critical for controlling water-column irradiance, has also been suggested as an important control of phytoplankton standing crop in the region. For example, the mixing of warm subtropical waters southwards across the SSTC has been suggested to provide thermal stability to the water column and therefore, through shallower mixing, increased light availability (Longhurst, 1998; Llido et al., 2005).

The current paper reports data on phytoplankton photophysiology and community structure from a South Atlantic cruise encountering strong gradients in nutrient environments during two crossings of the SSTC. These data, together with the results from a suite of 24 h Fe addition incubation experiments, offer an improved knowledge of the phytoplankton standing crop, community structure, and photophysiology in the region,

BGD
10, 11969–12008, 2013

in addition to providing strong field evidence for the dominant controls on FRRf signals in these regimes. The detailed sections of photophysiological parameters along the transect, together with supporting ancillary data, clearly demonstrate how the system is controlled by the contrasting conditions of low macronutrient, subtropical gyre-type waters and low Fe, high macronutrient sub-Antarctic ACC waters.

2 Methods

2.1 General

2.1.1 Cruises

Data was collected on the 68th cruise of the RRS James Cook (JC068), as Section GA10 of the GEOTRACES programme. The cruise took place in mid-austral summer (28 December 2011–25 January 2012) and followed a track, mostly at 40° S, occupying 21 stations between Cape Town, South Africa and Montevideo, South America (Fig. 1a). One station (Station 9) was occupied immediately to the east (i.e. downstream) of Gough Island – a volcanic island situated at 40.32° S, 9.92° W.

2.1.2 CTD data

Vertical profiles of temperature, salinity, fluorescence and (occasionally) photosynthetically available radiation (PAR) were collected using a Seabird 911 CTD. Mixed-layer depths (MLD) were calculated using the threshold method of de Boyer Montégut et al. (2004). In this method, the MLD is identified as the depth at which density changes by a threshold value (0.125 $kg\,m^{-3}$) relative to one at a near-surface reference depth (10 m). A linear interpolation between observed levels is then used to estimate the exact depth at which the difference criterion is met (de Boyer Montégut et al., 2004; Suga et al., 2004). Using this finite difference criterion has been shown to better represent the MLD compared to integral and regression methods (Thomson and Fine, 2003;

BGD
10, 11969–12008, 2013

de Boyer Montégut et al., 2004). The euphotic depth (z_{eu}) was calculated from PAR profiles and is here defined as the depth at which PAR reduced to 1 % of values at the surface. At stations where no PAR profiles were obtained, a correlation between chlorophyll and the diffuse attenuation coefficient K_d (calculated from profiles where PAR was collected) was used to estimate K_d and therefore z_{eu} using $z_{eu} = 4.6/K_d$.

2.1.3 Remote sensing

To examine the spatial and temporal variability in both chlorophyll *a* and sea surface temperature (SST), and to monitor how the boundaries of the ACC and subtropical gyre provinces varied over the sampling period, satellite images from the Moderate Resolution Imaging Spectroradiometer (MODIS) were downloaded in daily, three day, eight day and monthly composite formats from the ocean colour website (http://oceancolor.gsfc.nasa.gov/).

2.2 Nutrient concentrations

2.2.1 Macronutrients

The dissolved macronutrients silicate, phosphate and nitrate + nitrite (hereafter simply referred to as nitrate) were analyzed on-board ship using a micromolar Bran and Luebbe AAIII segmented flow, colorimetric autoanalyser with 4 analytical channels (nitrate + nitrite, nitrite, phosphate, silicate), using methods described in Woodward and Rees (2001). The results were checked against a certified nutrient reference material, made by KANSO Technos, Japan. Clean analytical, handling and sampling techniques were employed according to the GO-SHIP repeat hydrography manual (Hydes et al., 2010).

BGD
10, 11969–12008, 2013

2.2.2 Trace metal concentrations

Surface seawater samples for trace metal analysis and incubation experiments were pumped from a towed fish at a depth of 2 to 3 m. The seawater was pumped to a trace metal clean sampling container via a completely enclosed system with the suction provided by a Teflon diaphragm pump. Samples were filtered in-line through a 0.2 µm cartridge filter (AcroPak1000™) directly into acid cleaned low density polyethylene (LDPE) sample bottles. Discrete water samples from depth were obtained via 20 L Niskin sampling bottles deployed on a titanium frame CTD rosette using a Kevlar cable. Dissolved samples for trace metal analysis were collected after filtration through 0.2 µm cartridge filters (AcroPak500™), with slight overpressure provided by a clean air compressor.

Seawater samples for trace metal analysis were acidified with concentrated ultrapure hydrochloric acid (Romil, UpA) to pH 1.6 (0.023 M H^+), and shipped to the National Oceanography Centre (Southampton, UK). Trace metal samples were analyzed under clean air conditions using a modified method previously outlined by Milne et al. (2010) using isotope dilution inductively coupled plasma mass spectrometry (ID-ICP/MS (Thermo Element XR)). To validate analyzed sample concentrations, seawater standards (SAFe and GEOTRACES) were analyzed with each batch of samples. Values agreed within the consensus values for SAFe and GEOTRACES (SAFe S: 0.09 ± 0.03 nmol Fe kg^{-1} (consensus 0.09 ± 0.01 nmol Fe kg^{-1}), GEOTRACES GS: 0.56 ± 0.05 nmol Fe kg^{-1} (consensus 0.52 ± 0.07 nmol Fe kg^{-1})). The precision for replicate analyses was between 1–3 %. The manifold blank was 0.056 ± 0.016 nmol Fe kg^{-1}, and the limit of detection (3 × standard deviation of the blank) was determined to 0.032 ± 0.020 nmol Fe kg^{-1}.

BGD
10, 11969–12008, 2013

2.3 Phytoplankton community structure

2.3.1 Accessory pigment composition

Samples for High Performance Liquid Chromatography (HPLC) (0.5–2 L) were filtered onto 0.7 µm Whatman GF/F filters which were immediately flash-frozen in liquid nitrogen and then stored in a −80 °C freezer. Pigments were extracted into 90 % acetone by sonification and then analyzed using a Thermo HPLC system following the method described in Gibb et al. (2000). Pigments were identified using diagnostic retention times and comparison of individual pigment absorption spectra from a known spectral library. Chlorophyll *a* and pigment mixture standards were included in each run to calibrate retention times for the accessory pigments.

2.3.2 Phytoplankton absorption spectra

Phytoplankton absorption samples were collected by filtering 0.5–1 L seawater onto GF/F filters and flash-freezing the filter papers in liquid nitrogen before transfer to a −80 °C freezer for storage. Measurements were made using the hot methanol extraction method of Kishino (1985) using a Shimadzu UV-2550 spectrophotometer equipped with an integrating sphere over the visible range (350–750 nm). Optical densities for total (i.e. prior to methanol extraction) and detrital (after extraction) particles were corrected for optical pathlength amplification arising from scattering caused by the filter, according to the method of Cleveland and Weidemann (1993). Phytoplankton absorption coefficients (a_{ph}) were calculated by subtracting the detrital absorption spectra from the total absorption spectra. Pigment-specific absorption coefficients (a^*_{ph}) were calculated by dividing a_{ph} by the HPLC-determined chlorophyll *a* concentration.

2.3.3 Flow cytometric analysis

Concentrations of nanophytoplankton, photosynthetic picoeukaryotes (PPEs), *Synechococcus*, *Prochlorococcus*, and total heterotrophic bacteria were analyzed by ana-

BGD
10, 11969–12008, 2013

lytical flow cytometry (AFC). Samples (2 mL) were fixed with neutralized paraformaldehyde (1 % final concentration) and left for 10 min in the dark at room temperature before being flash-frozen in liquid nitrogen. Samples were then transported and stored in a −80 °C freezer prior to AFC analysis.

Samples were thawed at room temperature and analyzed using a FACSort flow cytometer (Becton Dickenson, Oxford, UK) according to the methods described in Davey et al. (2008) and Zubkov et al. (2003). An aliquot of sample (500 µL) was stained with 50 µL of 1 % SYBR Green 1 DNA dye (SYBR Green diluted 100× in potassium citrate) for identification of total bacteria. Half of the remaining 1.5 mL was used for the purpose of identifying *Synechoccocus*, PPEs, and nanophytoplankton, and the other half for identifying *Prochlorococcus*. The FACsort instrument counted particles and measured chlorophyll fluorescence (> 650 nm), orange fluorescence (585 ± 21 nm), SYBR Green fluorescence, and side scatter (light scattered at 90 ° to the plane of vertically polarized argon ion laser exciting at 488 nm). Samples were analyzed in duplicate for 3 min at a flow rate of ∼ 170 µL min^{-1} for counts of nanophytoplankton, PPEs, *Synechococcus*, and *Prochlorococcus*. SYBR Green stained samples were analyzed for 1 min at a flow rate of ∼ 60 µL min^{-1} for counts of total bacteria.

Data analysis and cell counts were carried out in WinMDI Version 2.8 (Joseph Trotter) flow cytometry analysis software. Scatter plots of orange fluorescence versus red fluorescence were used to discriminate and enumerate *Synechococcus* from other pico- and nanophytoplankton, and plots of side scatter versus red fluorescence (with *Synechococcus* gated out) were used to enumerate PPEs and nanophytoplankton. Plots of side scatter versus orange fluorescence were then used to gate out *Synechococcus* from plots of side scatter versus red fluorescence which were then used to enumerate *Prochlorococcus.* Total bacteria were enumerated from plots of side scatter versus SYBR Green fluorescence.

BGD
10, 11969–12008, 2013

2.4 Fast Repetition Rate fluorometry

A Fast Repetition Rate fluorometer (FRRf) (FAST$^{tracka\,//}$ with integrated FAST^{act} base unit, Chelsea Technologies Group Ltd.) was used to make measurements of phytoplankton photophysiology on samples from multiple depths in the euphotic zone. In a single acquisition protocol, the FRRf was set to deliver 64 sequences of one hundred 1 µs saturation flashes at 1 µs intervals followed by twenty five 1 µs relaxation flashes at 84 µs intervals. Rapid Light Curves (RLC) were also run for all surface and subsurface chlorophyll maximum (SCM) samples. The RLC protocol was a series of identical FRRf single acquisitions (same settings as for single acquisitions, except sequences per acquisition were reduced to 32), performed under a series of 15 progressively higher PAR intensities ranging from 6 to 1434 µmol photons m^{-2} s^{-1} delivered from the integrated FAST^{act} system. Each illumination step in the RLC lasted for 180 s, with 10 s dark steps in between.

Samples were dark-acclimated in opaque plastic bottles for at least 30 min prior to analysis and maintained at sea surface temperature by incubating in a water bath of flowing seawater from the ship's underway system. Blanks were run for the majority of samples using the following procedure (after Cullen and Davis, 2003): an aliquot of roughly 3 mL of sample was gently filtered using a 0.2 µm pore size Nalgene syringe filter unit and a single acquisition FRRf measurement made using the same FRRf settings as the unfiltered sample. The average of fluorescence of a blank was taken (i.e. the mean fluorescence of 125 repetitions of the flash sequence). Minimal variable fluorescence was found in all sample blanks. All sample fluorescence values were subsequently blank-corrected by subtracting the blank from unfiltered samples before any further analysis.

Fluorescence transients were fit using the model of Kolber et al. (1998) in FASTpro (V1.5) software supplied with the instrument (Chelsea Technologies Group Ltd.). Parameter recovery using this software was checked against previous analysis methods performed in a MATLAB^{TM} environment using custom codes (Laney, 2003; Moore et al.,

BGD
10, 11969–12008, 2013

2006b; Moore, unpub.). F_v/F_m was calculated as $(F_m - F_o)/F_m$ (where F_o is the fluorescence at the zeroth flashlet and F_m is the maximum fluorescence), with functional absorption cross sections (σ_{PSII}) recovered from the fit to the model of Kolber et al. (1998), effectively corresponding to the initial gradient of the fluorescence transients. The decline in fluorescence during relaxation flashes in the FRRf single acquisition protocol represents plastoquinone Q_A re-oxidation in PSII, where the dominant decay component, τ_{QA}, represents the timescale of electron flow between plastoquinones A and B. Relative electron transport rates per RCII (ETR) were calculated from the RLC data using Eq. (1) (Gorbunov et al., 2001):

$$\mathrm{ETR} = E\,\sigma_{\mathrm{PSII}}\left(\frac{F'_q/F'_m}{F_v/F_m}\right) \quad (1)$$

where E is the ambient PAR intensity supplied by the FAST^{act} system, $F'_q = F'_m - F'_o$, and prime symbols indicate the measurements were made under actinic light. Calculated ETR's were then fitted to the following function (adapted from Platt et al., 1980):

$$\frac{\mathrm{ETR}}{E} = \left(\frac{\mathrm{ETR}_{\max}}{E}\right)\left(1 - e^{\left(\frac{-\alpha_{\mathrm{ETR}}E}{\mathrm{ETR}_{\max}}\right)}\right) \quad (2)$$

where ETR_{max} represents the maximum light saturated ETR plateau and α_{ETR} represents the gradient of the light-limited slope and will effectively be proportional to σ_{PSII}. Normalization of ETR to irradiance provides a more statistically robust fitting method (Silsbe and Kromkamp, 2012), particularly improving fit quality at high irradiance. The optimum light intensity E_k was calculated as $\mathrm{ETR}_{max}/\alpha_{ETR}$.

2.5 Incubation experiments

Nine trace metal-clean, 1 L polycarbonate bottles were filled with trace metal clean water either from the towed fish described previously or, for samples from the SCM, from

BGD
10, 11969–12008, 2013

the titanium frame CTD rosette (see Fig. 6a for depths). When sampling from the towed fish, bottles were filled close to midnight to avoid any effects of light stress on phytoplankton photophysiology. Three bottles were sub-sampled immediately for initial measurements of photophysiology and chlorophyll *a* concentrations. For all experiments, samples for chlorophyll *a* analysis (100 mL) were filtered onto 0.7 µm Whatman GF/F filter papers then extracted overnight in the dark in 10 mL 90 % acetone in a −20 °C freezer, before measurement on a calibrated Trilogy fluorometer (Turner designs) following the method of Holm-Hansen et al. (1965). Of the remaining six bottles, 3 were spiked with 200 µL $FeCl_3$ in a 10 % HCl solution resulting in a final Fe concentration of 2 nmol L^{-1} and 3 bottles were sealed immediately with no amendment. The 3 amended and 3 control (non amended) bottles were sealed around the lids with Parafilm™, double bagged, and placed in an on-deck incubator filled with continuously replenished sea-surface water from the ship's underway water system to limit temperature change of the samples. The incubator was light shaded with blue screening to simulate the light field at ∼ 5 m water depth.

After 24 h the bottles were sub-sampled for photophysiology and fluorometric chlorophyll *a* concentration. Iron-stressed waters were defined as those that produced a statistically significant ($p < 0.01$ level using a one-tailed Student's t test) F_v/F_m increase in the Fe-amended bottles over that of the control (non-amended) bottles. Values of $\Delta F_v/F_m$ were calculated, where $\Delta F_v/F_m$ = average F_v/F_m Fe amended bottles – average F_v/F_m control bottles (Ryan-Keogh et al., 2013). Chlorophyll *a* concentrations were not expected to increase in response to the amendments, as 24 h is too short a period for phytoplankton to display a significant biomass increase in response to relief of nutrient limitation (e.g. Greene et al., 1992; Ryan-Keogh et al., 2013). The short duration of our bottle experiments will minimize significant changes in the taxonomic composition of the phytoplankton community during the incubation, resulting in F_v/F_m differences likely being indicative of direct physiological changes only (Moore et al., 2008; Suggett et al., 2009; Ryan-Keogh et al., 2013).

BGD
10, 11969–12008, 2013

Samples for macronutrients (nitrate, phosphate and silicate) and trace metals were taken prior to the bottle filling procedure described above, and for some experiments macronutrient samples were also sub-sampled for each of the three initial bottles. No samples for macronutrients were taken after the 24 h incubation period as previous studies have shown insignificant changes, even where F_v/F_m responses are seen, due to the short nature of the incubation time (Ryan-Keogh et al., 2013). All sampling, sub-sampling, and Fe spiking was carried out using trace metal-clean techniques, either in a trace metal clean container on the ship or in a trace metal clean laminar flow hood in the ship laboratory (Fe spiking only).

3 Results

3.1 General hydrography

The SSTC can be traced almost continuously around the globe between 35–45° S and divides the anticyclonic circulation of the Southern Hemisphere gyres from the cyclonic circulation of the ACC. The convergence results in a region of strong downwelling and sharp surface temperature and salinity gradients (Fig. 1; Lutjeharms, 1985). The SSTC has been defined operationally as a band of elevated chlorophyll concentrations (0.2–0.3 mg chlorophyll *a* m^{-3}, Longhurst, 1998), although this becomes poorly constrained in the Western Atlantic. A more practical definition for the Atlantic sector of the SSTC is to use sea-surface temperature, with a contour of 16 °C corresponding well to the nutrient gradients associated with the two water masses involved (Figs. 1 and 2). The latitude of the SSTC is seasonally dependant, with flow rates of the Agulhas Current (AC) and the Brazil Current (BC) increasing in austral summer (Walker, 1986; Matano et al., 1993), resulting in a southward expansion of South Atlantic Gyre waters and a resultant southward shift in the SSTC. In the western basin, the southward shift in the intersection point of the BC and Malvinas Current (MC) (the BC-MC confluence) in austral summer has been shown to be caused by an acceleration of water flow in the

BGD
10, 11969–12008, 2013

subtropical gyre and a weakened MC (Matano et al., 1993). Mixed-layer depths show consistent values of between ~ 40–60 m throughout the central basin (40° W to 15° E), reducing to < 25 m nearer South African and South American coasts (Fig. 1b).

3.2 Nutrients

3.2.1 Macronutrients

Concentrations of nitrate and phosphate were depleted (< 0.3 µmol L^{-1} nitrate) in surface waters (0–50 m), and higher (5–12 µmol L^{-1} nitrate) at greater depths, apart from in the sub-Antarctic ACC waters south of the SSTC in the eastern basin where elevated concentrations (~ 5 µmol L^{-1} nitrate) were seen to extend into the surface waters (Fig. 2a and b). Concentrations of silicate were uniformly low (< 1 µmol L^{-1}) in surface waters (~ 0–50 m depth) apart from near the South African and American coasts where they increase to higher concentrations (Fig. 2c).

3.2.2 Micronutrients

Dissolved Fe concentrations (DFe) showed low but variable surface concentrations throughout the cruise track (0.083 to 0.535 nmol L^{-1}, Fig. 2d). Consistently low concentrations (< 0.16 nmol L^{-1}) were seen in the surface AC and sub-Antarctic ACC waters in the Eastern Atlantic. To the west of 33° W concentrations were more variable but generally higher, with maximal values approaching South America, reaching a high of 0.535 nmol L^{-1} in close proximity to the Plata River.

3.3 Chlorophyll *a* concentrations

Satellite images show surface chlorophyll concentrations in the SSTC which are typically elevated with respect to waters further north (Southern Hemisphere subtropical gyres) and south (the ACC) throughout the year, although peak concentrations are found during austral spring and summer (September to February) (Fig. 3a–f). The band

BGD
10, 11969–12008, 2013

of elevated chlorophyll coinciding with the SSTC shows a southward shift in austral summer associated with increased AC and BC flow and a resultant southward expansion of the subtropical gyre (Fig. 3). In association with the trajectory of the SSTC (which occupies lower latitudes in the eastern basin than the western basin, Fig. 1a), the band of elevated chlorophyll concentrations is typically found further north in the eastern portion of the basin. For example, peak chlorophyll concentrations at 40° S for the austral spring-summer of 2011–2012 are seen in November 2011 for the western basin (40° W to 20° W) and February 2012 for the eastern basin (10° W to 10° E).

Profiles of chlorophyll *a* concentrations revealed elevated and depth-uniform values (0.2–0.7 mg m^{-3}) within the mixed layer for sub-Antarctic ACC waters in the central eastern basin, whilst low surface concentrations (< 0.2 mg m^{-3}) and elevated deep concentrations (typically > 0.4 mg m^{-3} and reaching a maximum of 1.46 mg m^{-3}) are observed in the higher temperature regions of the western basin and nearer to the South African coast (Fig. 3a and b). Elevated mixed-layer chlorophyll *a* concentrations are seen at the station in close proximity to the Plata River (~ 0.7 to 0.9 mg m^{-3}).

3.4 Phytoplankton community structure

Specific absorption coefficients were low in the eastern basin in comparison with the rest of the transect (Fig. 4a), suggesting the presence of larger phytoplankton cells relative to the subtropical gyre-type regimes (Ciotti et al., 2002; Yentsch and Phinney, 1989). Correspondingly, AFC results showed higher concentrations of nanophytoplankton in the eastern basin (Fig. 4b). Elevated concentrations of smaller cells (picophytoplankton) are seen in these waters and at SCM depths in subtropical gyre-type waters, which also included elevated concentrations of *Synechococcus* and *Prochlorococcus* (Fig. 4d and e).

The AFC results generally agreed with the relative phytoplanktonic size fractions derived from diagnostic pigments from the HPLC analysis (Uitz et al., 2006). HPLC samples showed a dominance of 19′-hexanoyloxyfucoxanthin (19′-Hex) (Fig. 5g) in the eastern basin suggestive of a haptophyte-dominated community. To a lesser extent,

BGD
10, 11969–12008, 2013

19′-Hex also dominated diagnostic pigments in the western basin and closer to the South African coast, but the photoprotective pigment zeaxanthin (Fig. 5d), a diagnostic pigment of cyanobacteria, was also found to contribute significantly to the total pigment complement. Elevated concentrations of divinyl chlorophyll *a* (Fig. 5h) in some of these samples in the western basin were indicative of *Prochlorococcus*, matching with elevated *Prochlorococcus* abundances measured by AFC (Figs. 4e and 5 h). Elevated contributions of peridinin (Fig. 5a), the unambiguous marker pigment for dinoflagellates, were found in the eastern basin, yet its contribution to total diagnostic pigments generally remained only around 10 % in this region. High contributions of the photoprotective pigment diadinoxanthin (Fig. 5b) were found in surface waters across the whole transect, as has been observed in previous studies of haptophyte-dominated waters (e.g. Gibb et al., 2000, 2001). The highest fucoxanthin contributions (Fig. 5e) were observed in the stations furthest west along the cruise track within close proximity to the Plata River, suggestive of diatoms dominating these waters.

3.5 Phytoplankton photophysiology

The section of F_v/F_m in Fig. 6a shows strong variations in along-transect photophysiology, which again match up with the distinct regimes identified from previously described temperature, macronutrient, chlorophyll *a* and phytoplankton community data. Apart from the station sampled close to Gough Island (Station 9), low values of F_v/F_m ($F_v/F_m < 0.3$) are seen throughout the mixed layer in the sub-Antarctic ACC waters of the eastern basin, with increases at greater depths ($F_v/F_m > 0.3$). Conversely, higher values are seen at all depths in subtropical gyre-type waters in the western basin and in AC waters. Off the South African coast, small but clear F_v/F_m reductions occur at the SCM. Slightly more longitudinal variability was found in surface water (< 10 m) F_v/F_m values than for deeper samples. Values of σ_{PSII} showed a less clear trend than F_v/F_m (Fig. 6b), although a general trend of inverse co-variability with F_v/F_m can be discerned: higher values in the eastern basin than in the western basin and coastal waters are seen. Trends in $1/\tau_{QA}$ were not clear, with significant depth and longitudinal variability

BGD
10, 11969–12008, 2013

(not shown). Despite this there was some indication of reduced values in ACC waters south of the SSTC.

RLC parameters again showed a less clear spatial trend than F_v/F_m, yet some broad characteristics of the different regions can be discerned (Fig. 6c and d). Surface samples from thermally-stratified subtropical gyre-type waters show higher ETR_{max} and E_k values than SCM samples. Sub-Antarctic ACC waters south of the SSTC in the eastern basin show less variability between surface and SCM depths, and have ETR_{max} and E_k values in between that of the surface and SCM samples from subtropical waters. As expected, values of α_{ETR} followed trends in σ_{PSII} ($R^2 = 0.53$).

3.6 Fe addition experiments

The Fe addition experiments showed clear (*t* test $p < 0.01$) F_v/F_m responses from Fe-amended bottles over that of the control bottles for surface waters in the eastern basin between 10° E and 10° W (IF3 to IF8 in Fig. 7). Elsewhere no significant F_v/F_m response from Fe amendment was seen. Significant changes in chlorophyll *a* concentrations were not observed in the majority of experiments.

4 Discussion

4.1 Interpreting patterns of phytoplankton photophysiology in and around the SSTC

The section of F_v/F_m (Fig. 6a), together with ancillary chemical and phytoplankton data (Figs. 2–5) and the Fe incubation experiments (Fig. 7) demonstrates a clear division of this ocean section into two regimes: (1) low macronutrient, sufficient Fe, and higher F_v/F_m to the north of the SSTC; and (2) elevated macronutrient, lower Fe, and lower F_v/F_m to the south. Several factors are thought to control values of F_v/F_m, including light climate, the particular phytoplankton taxa present and the nutrient regime (Sug-

BGD
10, 11969–12008, 2013

gett et al., 2009). Using accessory pigment, AFC, irradiance and experimental data however, we can eliminate the first two controls and demonstrate that macronutrient and Fe availability govern the majority of variability in this parameter for our study region.

Light stress has been shown to result in photodamage to reaction centre proteins (e.g. Horton et al., 1996; Raven, 2011), or the down-regulation of PSII (e.g. Milligan et al., 2012). However, any resultant reductions in F_v/F_m might be expected to reduce F_v/F_m principally in the high irradiance surface of the stratified low macronutrient regions, rather than the ACC waters. Irrespectively light induced changes in F_v/F_m would also not explain the observed differences in F_v/F_m between experimental treatments (Fig. 7). The taxonomic composition of the phytoplankton community can potentially influence F_v/F_m signatures, with a general trend of decreasing F_v/F_m with decreasing cell size when grown under the same environmental conditions (Suggett et al., 2009). However, our a^*_{ph} and AFC data clearly demonstrate larger cells dominating in the low F_v/F_m region of the eastern basin, with a greater contribution of smaller cells in the higher F_v/F_m regions (Figs. 4 and 6a). Furthermore, the diagnostic pigments from this study are also consistent with phytoplankton taxa not being the principal control on F_v/F_m across this ocean transect, with pigments suggesting haptophytes, known to have intermediate F_v/F_m when grown under nutrient-replete conditions (Suggett et al., 2009 and references therein), dominating the majority of the transect, but particularly the low F_v/F_m ACC waters of the central eastern basin (Fig. 5). In contrast, cyanobacteria, which tend to display lower nutrient replete values of F_v/F_m (Suggett et al., 2009), were found to be more prevalent in the high F_v/F_m gyre-type waters (Figs. 5 and 6a). Further, in terms of the significant F_v/F_m responses from the Fe-addition experiments in the ACC waters south of the SSTC, net differential growth sufficient to generate taxonomic shifts in the bottles is unlikely over the short 24 h timescale (Moore et al., 2008; Ryan-Keogh et al., 2013), as evidenced by the generally insignificant changes in total chlorophyll *a*.

BGD
10, 11969–12008, 2013

Laboratory studies have demonstrated that macronutrient starvation can lead to reductions in F_v/F_m due to a reduction reaction centre functionality (e.g. Kolber et al., 1988; Geider et al., 1993b). However, this type of nutrient stress actually appears rare in the open ocean (although see Kolber et al., 1990; Geider et al., 1993a), where more steady-state macronutrient stress appears to result in maintained F_v/F_m values (MacIntyre et al., 1997; Parkhill et al., 2001; Behrenfeld et al., 2006; Kruskopf and Flynn, 2006; Moore et al., 2008; Schrader et al., 2011). The high F_v/F_m values observed in waters with nitrate concentrations of less than 0.02 µmol L^{-1} are consistent with such an interpretation (Figs. 2a and 6a). In contrast, Fe limitation both in terms of starvation and possibly steady-state limitation, has been observed to result in depressed values of F_v/F_m which is relieved upon the addition of Fe, both in culture (Geider et al., 1993b; Greene, 1991, 1992; Vassiliev et al., 1995; Sharader et al., 2011) and in situ (Greene, 1994; Kolber, 1994; Vassiliev et al., 1995; Behrenfeld, 1996; Olson, 2000; Boyd and Abraham, 2001; Sosik and Olson, 2002; Moore, 2007) although note that high F_v/F_m was observed under steady-state Fe-limited diatom cultures by Peers and Price (2004). In a similar manner, our observations of F_v/F_m recovery south of the SSTC after Fe enrichment (Fig. 7), together with a step-wise elimination of the other potential controls discussed above, allows us to confidently ascribe the observed low F_v/F_m values to Fe stress.

Two mechanisms have been put forward to explain depressed F_v/F_m values in Fe-limited waters. Firstly, as Fe is an essential component of the photosynthetic apparatus, its absence could potentially limit the functionality of PSII reaction centres (e.g. Greene et al., 1994; Kolber et al., 1994). However, more recent work has suggested that low F_v/F_m values may originate from the production of excess disconnected light harvesting centres (DLHC) under conditions of Fe-limited growth (Behrenfeld et al., 2006; Schrader et al., 2011; Ryan-Keogh et al., 2012; Fraser et al., 2013). Excess pigments energetically uncoupled from a functional reaction centre will not contribute to photochemistry but could contribute to total fluorescence (i.e. increase F_o and F_m), and hence reduce F_v/F_m independently of F_v (Schrader et al., 2011; Ryan-Keogh et al.,

BGD
10, 11969–12008, 2013

2012). As such, depressed values of F_v/F_m would characterize a Fe-stress physiological response, but without any coincident dysfunctionality of reaction centres or impairment of carbon fixation efficiencies (Behrenfeld and Milligan, 2013). Consequently, depressed F_v/F_m in the sub-Antarctic waters south of the SSTC may still correspond to conditions of balanced Fe limitation of the phytoplankton standing crop, in a similar manner to the expected macronutrient limitation of waters to the north of the front.

The data collected in this study provides clear field evidence that high F_v/F_m signatures can be produced in low Fe waters provided that coincident low macronutrient concentrations are found (compare Fig. 2a, b, d with Fig. 6a and also see Fig. 8). For example, AC waters in the east of the cruise track show $F_v/F_m > 0.5$ yet DFe concentrations are less than 0.16 nmol L^{-1}. There is some evidence from laboratory experiments that Fe-macronutrient co-limited phytoplankton show elevated F_v/F_m (Schrader et al., 2011). This observation together with subsequent F_v/F_m reductions following macronutrient re-supply have been suggested to be due to the macronutrient requirement for DLHC synthesis (Schrader et al., 2011). With our current suite of experiments it is not possible to conclude whether or not the waters of the AC were Fe-macronutrient co-limited, although the addition of fixed nitrogen would likely have been required to stimulate any significant increase in the standing crop of phytoplankton.

More generally, these results also suggest that Fe-stressed conditions may not easily be identified solely on the basis of DFe concentrations (compare Fig. 2d with Fig. 6a, and also see Fig. 8). Measurements of DFe include soluble, colloidal, inorganic and ligand-bound fractions and considerable uncertainty persists as to the relative bioavailability of these fractions to phytoplankton (Shaked and Lis, 2012 and references therein). For the same measured DFe concentration, the ability for the available Fe to support the growth of the extant phytoplankton population might be expected to be higher in the subtropical gyre-type waters encountered compared with the ACC waters both as a result of the lower phytoplankton standing stock reducing competition for the metal and the generally smaller cell sizes increasing surface-area-to-volume ratios and hence the kinetics of metal uptake (Hudson and Morel, 1990; Shaked et al., 2005).

BGD
10, 11969–12008, 2013

Whilst at the level of an individual phytoplankton cell the factors controlling Fe limitation are complex, our data support suggestions that regions of Fe limitation are characterizable on the basis of the relative supply of DFe and nitrate (Parekh et al., 2005). Loss of Fe to scavenging in the deep ocean results in waters upwelling from depth (such as occurs strongly within the ACC) having lower DFe : nitrate ratios than that of phytoplankton requirements (Johnson et al., 1997; Ito et al., 2005; Parekh et al., 2005; Sunda, 2012). Formation and subsequent export of organic material would therefore be expected to deplete Fe to levels that are limiting to phytoplankton growth in such regions. In contrast depletion of macronutrients under weaker replenishment from depth in subtropical gyre waters, alongside some level of external Fe supply (for example from dust), results in the gradual development of macronutrient limitation (Moore et al., 2013). Accordingly, across-transect values of the surface DFe : nitrate ratio suggested a good spatial correlation with both F_v/F_m and the proximal response of the phytoplankton community to Fe replenishment as indicated by $\Delta F_v/F_m$ in our study region (Fig. 8). Moreover the degree of Fe stress showed a stronger spatial relationship with both DFe : nitrate and even nitrate than with DFe (Fig. 8). Similarly Fe : macronutrient supply ratios effectively dictate the broad patterns of nutrient limitation which develop in regional (Ito et al., 2005) and global (Aumont et al., 2003; Moore et al., 2004) biogeochemical models. For example, the derived parameter Fe*, the difference between DFe and phosphate concentrations weighted by an assumed biological uptake ratio of the two nutrients ($R_{F:P}$), has been used to delineate Fe or macronutrient limited regions (Ito et al., 2005; Parekh et al., 2005).

Values of σ_{PSII} broadly show an inverse relationship to F_v/F_m (Fig. 6b), potentially indicating either larger connected LHC's and/or less operational reaction centres per LHC under Fe stressed conditions (Vassiliev et al., 1995; Behrenfeld and Milligan, 2013). The less clear spatial pattern of σ_{PSII} than for F_v/F_m may result from an enhanced taxonomic signature for this physiological trait (Suggett et al., 2004, 2009; Moore et al., 2005, 2006b). RLC parameters showed a less clear across-transect trend than F_v/F_m, instead being dominated by vertical gradients within the gyre-type waters,

BGD
10, 11969–12008, 2013

likely related to photoacclimation (Fig. 6c and d). In particular, elevated ETR_{max} and E_k of surface samples compared to SCM samples from subtropical gyre-type waters likely reflected acclimation to the increased irradiance encountered here. In contrast, RLC parameters displayed less vertical variability in ACC waters of the eastern basin, where values of ETR_{max} and E_k were in between that of the surface and SCM samples from the subtropical gyre-type regions to the east and west. Such a pattern likely resulted from more vigorous mixing in these waters and hence photoacclimation to a more dynamic light regime.

4.2 Controls on the development of the SSTC bloom

Satellite images suggest a diffuse band of elevated chlorophyll concentrations around the SSTC in austral summer (Fig. 3a–f). Increased irradiance in austral spring-summer, together with reduced mixed-layer depths (de Boyer Montégut et al., 2004), cause the increase in chlorophyll concentrations observed throughout the SSTC between September and February. Accompanying this increase, however, is a narrowing of the SSTC chlorophyll band which is suggested to be caused by the bloom-induced depletion of macronutrients to the north of the SSTC and Fe to the south. The SSTC itself represents a nutrient regime boundary, whereby unconsumed Fe in subtropical waters and macronutrients in ACC waters may mix to provide suitable conditions to maintain an elevated standing crop of phytoplankton (Ito et al., 2005). The wider SSTC chlorophyll band in the western basin is suggested to reflect continental nutrient supply from South America, specifically Fe to ACC waters south of the SSTC and Fe and macronutrients to the north.

Our results have revealed Fe-stressed phytoplankton within the austral summer SSTC chlorophyll band in the Eastern Atlantic. Variable fluxes of Fe to this region can therefore be speculated to control the phytoplankton crop in the region. This is particularly well demonstrated by natural Fe enrichment from Gough Island, which sits centrally in the Atlantic Basin at 40° S within the region of Fe limitation (Fig. 8). The eastward-flowing surface currents pass over the shallow-subsurface topography sur-

BGD
10, 11969–12008, 2013

rounding the island, and weathered material is presumably transported off the island by streams and as windblown dust. Evidence for Fe delivery to waters surrounding Gough Island comes from increased DFe, similar to other islands which have been hypothesized or shown directly to supply Fe to HNLC waters, for example the Crozet Islands (Planquette et al., 2007) and Kerguelen (Blain et al., 2001, 2002, 2007; Bucciarelli et al., 2001). Indeed, both elevated chlorophyll *a* concentrations and a recovery of F_v/F_m to higher values were observed for the single station occupied in the vicinity of Gough Island, as might be expected upon relief of Fe limitation. Fe fertilization by Gough Island appears spatially limited, the station just north of Gough Island (Station 8) showing no significant increases in chlorophyll *a* concentrations or F_v/F_m and the downstream (longitudinal) Fe-fertilization distance from Gough Island thus remains to be tested.

5 Conclusions

FRRf measurements of phytoplankton photophysiology alongside chlorophyll *a* concentrations, community structure, macronutrients and DFe, together with results from a suite of 24 h Fe-addition incubation experiments from a cruise in the South Atlantic, have characterized two regimes on the basis of nutrient limitation. The primary limiting nutrient of the elevated chlorophyll, relatively larger cell-dominated sub-Antarctic ACC waters south of the SSTC in the Eastern Atlantic Basin in mid-austral summer has been shown to be Fe. Increasing Fe availability in this region results in increased F_v/F_m values (bottle enrichment experiments and natural enrichment from Gough Island) and chlorophyll *a* concentrations (natural enrichment from Gough Island). To the north of the SSTC, as seen close to the South African coast and in the western section of the cruise transect, the phytoplankton standing crop showed elevated F_v/F_m and an enhanced contribution of smaller cells which are hypothesized to be limited by macronutrient availability.

BGD
10, 11969–12008, 2013

Our results indicated poorer spatial correlation of DFe with values of F_v/F_m than with DFe : nitrate ratios. Interestingly, the boundary between Fe-stressed and non-stressed regions was associated with a DFe : nitrate ratio of between 4×10^{-4} and 5×10^{-3} mol : mol, which is comparable with the extended average Redfield phytoplankton requirements of $\sim 1 \times 10^{-3}$ mol : mol (Quigg et al., 2011). Phytoplankton cells should not be directly sensitive to the local ratio of potentially limiting nutrients, responding rather to absolute availability (Moore et al., 2013). Consequently, as in other systems (Hutchins et al., 1998; Moore et al., 2006; Ryan-Keogh et al., 2013) and theoretical studies (Parekh et al., 2005; Ito et al., 2005), the observed relationship of Fe stress with DFe : nitrate likely reflects large-scale controls on upper ocean nutrient limitation generated by gradients in relative nutrient supply ratios (Ito et al., 2005). Moreover, future work on physiological responses to changing nitrate availability under conditions close to those where Fe is potentially co-limiting (Ryan-Keogh et al., 2013) might allow further assessment of whether F_v/F_m reductions following nitrate additions reflect co-limitation of phytoplankton by Fe and nitrate (Schrader et al., 2011) or simply a transition across a tipping point from nitrate to Fe limitation. Our results also suggested that other factors, including bioavailability, community structure, macronutrient availability and subsequent overall biological demand likely need to be considered alongside absolute DFe concentrations when assessing the potential for the development of regional Fe limitation. Such considerations may be particularly pertinent as the global coverage of DFe data increases rapidly though the GEOTRACES programme.

Acknowledgements. We thank the officers, crew, technicians and scientists of the RRS James Cook for their help on the UK-GEOTRACES JC068 cruise. This work was funded by the UK-GEOTRACES National Environment Research Council (NERC) Consortium Grant (NE/H006095/1) which included a studentship to T. J. B.

BGD
10, 11969–12008, 2013

References

Aumont, O., Maier-Reimer, E., Blain, S., and Monfray, P.: An ecosystem model of the global ocean including Fe, Si, P colimitations, Global Biogeochemical Cy., 17, 1060, doi:10.1029/2001gb001745, 2003.

Behrenfeld, M. J. and Falkowski, P. G.: Photosynthetic rates derived from satellite-based chlorophyll concentration, Limnol. Oceanogr., 42, 1–20, 1997.

Behrenfeld, M. J. and Milligan, A. J.: Photophysiological expressions of iron stress in phytoplankton, Annu. Rev. Mar. Sci., 5, 217–246, doi:10.1146/annurev-marine-121211-172356, 2013.

Behrenfeld, M. J., Bale, A. J., Kolber, Z. S., Aiken, J., and Falkowski, P. G.: Confirmation of iron limitation of phytoplankton photosynthesis in the equatorial Pacific Ocean, Nature, 383, 508–511, 1996.

Behrenfeld, M. J., Worthington, K., Sherrell, R. M., Chavez, F. P., Strutton, P., McPhaden, M., and Shea, D. M.: Controls on tropical Pacific Ocean productivity revealed through nutrient stress diagnostics, Nature, 442, 1025–1028, doi:10.1038/nature05083, 2006.

Blain, S., Treguer, P., Belviso, S., Bucciarelli, E., Denis, M., Desabre, S., Fiala, M., Jezequel, V. M., Le Fevre, J., Mayzaud, P., Marty, J. C., and Razouls, S.: A biogeochemical study of the island mass effect in the context of the iron hypothesis: Kerguelen Islands, Southern Ocean, Deep-Sea Res. Pt. I, 48, 163–187, doi:10.1016/s0967-0637(00)00047-9, 2001.

Blain, S., Sedwick, P. N., Griffiths, F. B., Queguiner, B., Bucciarelli, E., Fiala, M., Pondaven, P., and Treguer, P.: Quantification of algal iron requirements in the Subantarctic Southern Ocean (Indian sector), Deep-Sea Res. Pt. II, 49, 3255–3273, doi:10.1016/s0967-0645(02)00082-6, 2002.

Blain, S., Queguiner, B., Armand, L., Belviso, S., Bombled, B., Bopp, L., Bowie, A., Brunet, C., Brussaard, C., Carlotti, F., Christaki, U., Corbiere, A., Durand, I., Ebersbach, F., Fuda, J.-L., Garcia, N., Gerringa, L., Griffiths, B., Guigue, C., Guillerm, C., Jacquet, S., Jeandel, C., Laan, P., Lefevre, D., Lo Monaco, C., Malits, A., Mosseri, J., Obernosterer, I., Park, Y.-H., Picheral, M., Pondaven, P., Remenyi, T., Sandroni, V., Sarthou, G., Savoye, N., Scouarnec, L., Souhaut, M., Thuiller, D., Timmermans, K., Trull, T., Uitz, J., van Beek, P., Veldhuis, M., Vincent, D., Viollier, E., Vong, L., and Wagener, T.: Effect of natural iron fertilization on carbon sequestration in the Southern Ocean, Nature, 446, 1070–1074, doi:10.1038/nature05700, 2007.

BGD
10, 11969–12008, 2013

Boyd, P. W. and Abraham, E. R.: Iron-mediated changes in phytoplankton photosynthetic competence during SOIREE, Deep-Sea Res. Pt. II, 48, 2529–2550, 2001.
Boyd, P. W., Watson, A. J., Law, C. S., Abraham, E. R., Trull, T., Murdoch, R., Bakker, D. C. E., Bowie, A. R., Buesseler, K. O., Chang, H., Charette, M., Croot, P., Downing, K., Frew, R., Gall, M., Hadfield, M., Hall, J., Harvey, M., Jameson, G., LaRoche, J., Liddicoat, M., Ling, R., Maldonado, M. T., McKay, R. M., Nodder, S., Pickmere, S., Pridmore, R., Rintoul, S., Safi, K., Sutton, P., Strzepek, R., Tanneberger, K., Turner, S., Waite, A., and Zeldis, J.: A mesoscale phytoplankton bloom in the polar Southern Ocean stimulated by iron fertilization, Nature, 407, 695–702, doi:10.1038/35037500, 2000.
Boyd, P. W., Strzepek, R., Fu, F. X., and Hutchins, D. A.: Environmental control of open-ocean phytoplankton groups: Now and in the future, Limnol. Oceanogr., 55, 1353–1376, doi:10.4319/lo.2010.55.3.1353, 2010.
Bucciarelli, E., Blain, S., and Treguer, P.: Iron and manganese in the wake of the Kerguelen Islands (Southern Ocean), Mar. Chem., 73, 21–36, doi:10.1016/s0304-4203(00)00070-0, 2001.
Ciotti, A. M., Lewis, M. R., and Cullen, J. J.: Assessment of the relationships between dominant cell size in natural phytoplankton communities and the spectral shape of the absorption coefficient, Limnol. Oceanogr., 47, 404–417, 2002.
Cleveland, J. S. and Weidemann, A. D.: Quantifying absorption by aquatic particles – a multiple-scattering correction for glass-fiber filters, Limnol. Oceanogr., 38, 1321–1327, 1993.
Cullen, J. J. and Davis, R. F.: The blank can make a big difference in oceanographic measurements, Limnol. Oceanogr. Bull., 12, 29–35, 2003.
Cullen, J. J., Yang, X., Macintyre, H. L.: Nutrient limitation of marine photosynthesis, in: Primary Productivity and Biogeochemical Cycles in the Sea, edited by: Falkowski, P. G. and Woodhead, A., Plenum, 69–88, 1992.
Davey, M., Tarran, G. A., Mills, M. M., Ridame, C., Geider, R. J., and LaRoche, J.: Nutrient limitation of picophytoplankton photosynthesis and growth in the tropical North Atlantic„ Limnol. Oceanogr., 53, 1722–1733, doi:10.4319/lo.2008.53.5.1722, 2008.
Dugdale, R. C. and Goering, J. J.: Uptake of new and regenerated forms of nitrogen in primary productivity, Limnol. Oceanogr., 12, 196–206, doi:10.4319/lo.1967.12.2.0196, 1967.
Eppley, R. W. and Peterson, B. J.: Particulate organic-matter flux and planktonic new production in the deep ocean, Nature, 282, 677–680, doi:10.1038/282677a0, 1979.

BGD
10, 11969–12008, 2013

Fraser, J. M., Tulk, S. E., Jeans, J. A., Campbell, D. A., Bibby, T. S., and Cockshutt, A. M.: Photophysiological and photosynthetic complex changes during iron starvation in *Synechocystis* sp. PCC 6803 and *Synechococcus elongatus* PCC 7942, PLoS ONE, 8, e59861, doi:10.1371/journal.pone.0059861, 2013.

Geider, R. J., Greene, R. M., Kolber, Z., Macintyre, H. L., and Falkowski, P. G.: fluorescence assessment of the maximum quantum efficiency of photosynthesis in the Western North-Atlantic, Deep-Sea Res. Pt. I, 40, 1205–1224, 1993a.

Geider, R. J., Laroche, J., Greene, R. M., and Olaizola, M.: Response of the photosynthetic apparatus of *Phaeodactylum-tricornutum* (Bacillariophyceae) to nitrate, phosphate, or iron starvation, J. Phycol., 29, 755–766, 1993b.

Gibb, S. W., Barlow, R. G., Cummings, D. G., Rees, N. W., Trees, C. C., Holligan, P., and Suggett, D.: Surface phytoplankton pigment distributions in the Atlantic Ocean: an assessment of basin scale variability between 50° N and 50° S, Prog. Oceanogr., 45, 339–368, doi:10.1016/s0079-6611(00)00007-0, 2000.

Gibb, S. W., Cummings, D. G., Irigoien, X., Barlow, R. G., Fauzi, R., and Mantoura, C.: Phytoplankton pigment chemotaxonomy of the northeastern Atlantic, Deep-Sea Res. Pt. II, 48, 795–823, doi:10.1016/s0967-0645(00)00098-9, 2001.

Gorbunov, M. Y., Kolber, Z. S., Lesser, M. P., and Falkowski, P. G.: Photosynthesis and photoprotection in symbiotic corals, Limnol. Oceanogr., 46, 75–85, doi:10.4319/lo.2001.46.1.0075, 2001.

Greene, R. M., Geider, R. J., and Falkowski, P. G.: Effect of iron limitation on photosynthesis in a marine diatom, Limnol. Oceanogr., 36, 1772–1782, 1991.

Greene, R. M., Geider, R. J., Kolber, Z., and Falkowski, P. G.: Iron-induced changes in light harvesting and photochemical energy-conversion processes in eukaryotic marine-algae, Plant Physiol., 100, 565–575, 1992.

Greene, R. M., Kolber, Z. S., Swift, D. G., Tindale, N. W., and Falkowski, P. G.: Physiological limitation of phytoplankton photosynthesis in the Eastern Equatorial Pacific determined from variability in the quantum yield of fluorescence, Limnol. Oceanogr., 39, 1061–1074, 1994.

Holm-Hansen, O., Lorenzen, C. J., Holmes, R. W., and Strickland, J. D. H.: Fluorometric determination of chlorophyll, J. Cons. Perm. Int. Explor. Mer., 30, 3–15, 1965.

Horton, P., Ruban, A. V., and Walters, R. G.: Regulation of light harvesting in green plants, Annu. Rev. Plant Phys., 47, 655–684, doi:10.1146/annurev.arplant.47.1.655, 1996.

BGD
10, 11969–12008, 2013

Hudson, R. J. M. and Morel, F. M. M.: Iron transport in marine phytoplankton: kinetics of cellular and medium coordination reactions, Limnol. Oceanogr., 35, 1002–1020, 1990.
Hutchins, D. A., DiTullio, G. R., Zhang, Y., and Bruland, K. W.: An iron limitation mosaic in the California upwelling regime, Limnol. Oceanogr., 43, 1037–1054, 1998.
Hydes, D. J., Aoyama, M., Aminot, A., Bakker, K., Becker, S., Coverly, S., Daniel, A., Dickson, A. G., Grosso, O., Kerouel, R., Van Ooijen, J., Sato, K., Tanhua, T., Woodward, E. M. S., and Zhang, J. Z.: Determination of dissolved nutrients (N, P, Si) in seawater with high precision and inter-comparability using gas-segmented continuous flow analysers, in: The GO-SHIP Repeat Hyrography Manual: a Collection of Expert Reports and Guidelines, IOCCP report No.14, ICPO publication series No. 134, version 1, 2010.
Ito, T., Parekh, P., Dutkiewicz, S., and Follows, M. J.: The antarctic circumpolar productivity belt, Geophys. Res. Lett., 32, L13604, doi:10.1029/2005gl023021, 2005.
Johnson, K. S., Gordon, R. M., and Coale, K. H.: What controls dissolved iron concentrations in the world ocean?, Mar. Chem., 57, 137–161, doi:10.1016/s0304-4203(97)00043-1, 1997.
Katz, M. E., Finkel, Z. V., Grzebyk, D., Knoll, A. H., and Falkowski, P. G.: Evolutionary trajectories and biogeochemical impacts of marine eukaryotic phytoplankton, Annu. Rev. Ecol. Evol. S., 35, 523–556, doi:10.1146/annurev.ecolsys.35.112202.130137, 2004.
Kishino, M., Takahashi, M., Okami, N., and Ichimura, S.: Estimation of the spectral absorption-coefficients of phytoplankton in the sea, B. Mar. Sci., 37, 634–642, 1985.
Kolber, Z. S., Zehr, J., and Falkowski, P.: Effects of growth irradiance and nitrogen limitation on photosynthetic energy conversion in photosystem-II, Plant Physiol., 88, 923–929, 1988.
Kolber, Z. S., Wyman, K. D., and Falkowski, P. G.: Natural variability in photosynthetic energy-conversion efficiency – a field-study in the Gulf of Maine, Limnol. Oceanogr., 35, 72–79, 1990.
Kolber, Z. S., Barber, R. T., Coale, K. H., Fitzwater, S. E., Greene, R. M., Johnson, K. S., Lindley, S., and Falkowski, P. G.: Iron limitation of phytoplankton photosynthesis in the Equatorial Pacific-Ocean, Nature, 371, 145–149, 1994.
Kolber, Z. S., Prasil, O., and Falkowski, P. G.: Measurements of variable chlorophyll fluorescence using fast repetition rate techniques: defining methodology and experimental protocols, BBA-Bioenergetics, 1367, 88–106, 1998.
Kruskopf, M. and Flynn, K. J.: Chlorophyll content and fluorescence responses cannot be used to gauge reliably phytoplankton biomass, nutrient status or growth rate, New Phytol., 169, 525–536, doi:10.1111/j.1469-8137.2005.01601.x, 2006.

BGD
10, 11969–12008, 2013

Laney, S. R.: Assessing the error in photosynthetic properties determined by fast repetition rate fluorometry, Limnol. Oceanogr., 48, 2234–2242, 2003.
Llido, J., Garcon, V., Lutjeharms, J. R. E., and Sudre, J.: Event-scale blooms drive enhanced primary productivity at the Subtropical Convergence, Geophys. Res. Lett., 32, L15611, doi:10.1029/2005gl022880, 2005.
Longhurst, A. R.: Ecological Geography of the Sea, Academic Press, San Diego, 1998.
Lutjeharms, J. R. E.: Location of frontal systems between Africa and Antarctica – some preliminary results, Deep-Sea Res. Pt. I, 32, 1499–1509, doi:10.1016/0198-0149(85)90100-1, 1985.
MacIntyre, J. G., Cullen, J. J., and Cembella, A. D.: Vertical migration, nutrition and toxicity in the dinoflagellate Alexandrium tamarense, Mar. Ecol.-Prog. Ser., 148, 201–216, doi:10.3354/meps148201, 1997.
Matano, R. P.: On the separation of the Brazil Current from the coast, J. Phys. Oceanogr., 23, 79–90, doi:10.1175/1520-0485(1993)023<0079:otsotb>2.0.co;2, 1993.
Milligan, A. J., Aparicio, U. A., and Behrenfeld, M. J.: Fluorescence and nonphotochemical quenching responses to simulated vertical mixing in the marine diatom Thalassiosira weissflogii, Mar. Ecol.-Prog. Ser., 448, 67–78, doi:10.3354/meps09544, 2012.
Milne, A., Landing, W., Bizimis, M., and Morton, P.: Determination of Mn, Fe, Co, Ni, Cu, Zn, Cd and Pb in seawater using high resolution magnetic sector inductively coupled mass spectrometry (HR-ICP-MS), Anal. Chim. Acta, 665, 200–207, doi:10.1016/j.aca.2010.03.027, 2010.
Montegut, C. D., Madec, G., Fischer, A. S., Lazar, A., and Iudicone, D.: Mixed layer depth over the global ocean: an examination of profile data and a profile-based climatology, J. Geophys. Res.-Oceans, 109, C102003, doi:10.1029/2004jc002378, 2004.
Moore, C. M., Lucas, M. I., Sanders, R., and Davidson, R.: Basin-scale variability of phytoplankton bio-optical characteristics in relation to bloom state and community structure in the Northeast Atlantic, Deep-Sea Res. Pt. I, 52, 401–419, doi:10.1016/j.dsr.2004.09.003, 2005.
Moore, C. M., Mills, M. M., Milne, A., Langlois, R., Achterberg, E. P., Lochte, K., Geider, R. J., and La Roche, J.: Iron limits primary productivity during spring bloom development in the central North Atlantic, Global Change Biol., 12, 626–634, doi:10.1111/j.1365-2486.2006.01122.x, 2006a.

BGD
10, 11969–12008, 2013

Moore, C. M., Suggett, D. J., Hickman, A. E., Kim, Y. N., Tweddle, J. F., Sharples, J., Geider, R. J., and Holligan, P. M.: Phytoplankton photoacclimation and photoadaptation in response to environmental gradients in a shelf sea, Limnol. Oceanogr., 51, 936–949, 2006b.

Moore, C. M., Seeyave, S., Hickman, A. E., Allen, J. T., Lucas, M. I., Planquette, H., Pollard, R. T., and Poulton, A. J.: Iron-light interactions during the CROZet natural iron bloom and EXport experiment (CROZEX) I: phytoplankton growth and photophysiology, Deep-Sea Res. Pt. II, 54, 2045–2065, doi:10.1016/j.dsr2.2007.06.011, 2007.

Moore, C. M., Mills, M. M., Langlois, R., Milne, A., Achterberg, E. P., La Roche, J., and Geider, R. J.: Relative influence of nitrogen and phosphorus availability on phytoplankton physiology and productivity in the oligotrophic sub-tropical North Atlantic Ocean, Limnol. Oceanogr., 53, 291–305, 2008.

Moore, C. M., Mills, M. M., Arrigo, K. R., Berman-Frank, I., Bopp, L., Boyd, P. W., Galbraith, E. D., Geider, R. J., Guieu, C., Jaccard, S. L., Jickells, T. D., La Roche, J., Lenton, T. M., Mahowald, N. M., Marañón, E., Marinov, I., Moore, J. K., Nakatsuka, T., Oschlies, A., Saito, M. A., Thingstad, T. F., Tsuda, A., and Ulloa, O.: Processes and patterns of oceanic nutrient limitation, Nat. Geosci., doi:10.1038/ngeo1765, 2013.

Moore, J. K., Doney, S. C., and Lindsay, K.: Upper ocean ecosystem dynamics and iron cycling in a global three-dimensional model, Global Biogeochem. Cy., 18, GB4028, doi:10.1029/2004gb002220, 2004.

Olson, R. J., Sosik, H. M., Chekalyuk, A. M., and Shalapyonok, A.: Effects of iron enrichment on phytoplankton in the Southern Ocean during late summer: active fluorescence and flow cytometric analyses, Deep-Sea Res. Pt. II, 47, 3181–3200, 2000.

Parekh, P., Follows, M. J., and Boyle, E. A.: Decoupling of iron and phosphate in the global ocean, Global Biogeochem. Cy., 19, GB2020, doi:10.1029/2004gb002280, 2005.

Parkhill, J. P., Maillet, G., and Cullen, J. J.: Fluorescence-based maximal quantum yield for PSII as a diagnostic of nutrient stress, J. Phycol., 37, 517–529, 2001.

Peers, G. and Price, N. M.: A role for manganese in superoxide dismutases and growth of iron-deficient diatoms, Limnol. Oceanogr., 49, 74–83, doi:10.4319/lo.2004.49.5.1774, 2004.

Planquette, H., Statham, P. J., Fones, G. R., Charette, M. A., Moore, C. M., Salter, I., Nedelec, F. H., Taylor, S. L., French, M., Baker, A. R., Mahowald, N., and Jickells, T. D.: Dissolved iron in the vicinity of the Crozet Islands, Southern Ocean, Deep-Sea Res. Pt. II, 54, 1999–2019, doi:10.1016/j.dsr2.2007.06.019, 2007.

BGD
10, 11969–12008, 2013

Platt, T., Gallegos, C. L., and Harrison, W. G.: Photoinhibition of photosynthesis in natural assemblages of marine-phytoplankton, J. Mar. Res., 38, 687–701, 1980.
Quigg, A., Irwin, A. J., and Finkel, Z. V.: Evolutionary inheritance of elemental stoichiometry in phytoplankton, P. Roy. Soc. B-Biol. Sci., 278, 526–534, doi:10.1098/rspb.2010.1356, 2011.
Raven, J. A.: The cost of photoinhibition, Physiol. Plantarum, 142, 87–104, doi:10.1111/j.1399-3054.2011.01465.x, 2011.
Ryan-Keogh, T. J., Macey, A. I., Cockshutt, A. M., Moore, C. M., and Bibby, T. S.: The cyanobacterial chlorophyll-binding protein IsiA acts to increase the in vivo effective absorption cross-section of PSI under iron limitation, J. Phycol., 48, 145–154, doi:10.1111/j.1529-8817.2011.01092.x, 2012.
Ryan-Keogh, T. J., Macey, A. I., Nielsdottir, M. C., Lucas, M. I., Steigenberger, S. S., Stinchcmbe, M. C., Achterberg, E. P., Bibby, T. S., and Moore, C. M.: Spatial and temporal development of phytoplankton iron stress in relation to bloom dynamics in the high-latitude North Atlantic Ocean, Limnol. Oceanogr., 58, 533–545, 2013.
Ryther, J. H. and Dunstan, W. M.: Nitrogen, phosphorous and eutrophication in coastal marine environment, Science, 171, 1008–1013, doi:10.1126/science.171.3975.1008, 1971.
Schrader, P. S., Milligan, A. J., and Behrenfeld, M. J.: Surplus photosynthetic antennae complexes underlie diagnostics of iron limitation in a cyanobacterium, Plos One, 6, e18753, doi:10.1371/journal.pone.0018753, 2011.
Shaked, Y. and Lis, H.: Disassembling iron availability to phytoplankton, Front. Microbiol., 3, 123, doi:10.3389/fmicb.2012.00123, 2012.
Shaked, Y., Kustka, A. B., and Morel, F. M. M.: A general kinetic model for iron acquisition by eukaryotic phytoplankton, Limnol. Oceanogr., 50, 872–882, 2005.
Silsbe, G. M. and Kromkamp, J. C.: Modeling the irradiance dependency of the quantum efficiency of photosynthesis, Limnol. Oceanogr.-Meth., 10, 645–652, doi:10.4319/lom.2012.10.645, 2012.
Sosik, H. M. and Olson, R. J.: Phytoplankton and iron limitation of photosynthetic efficiency in the Southern Ocean during late summer, Deep-Sea Res. Pt. I, 49, 1195–1216, 2002.
Suga, T., Motoki, K., Aoki, Y., and Macdonald, A. M.: The North Pacific climatology of winter mixed layer and mode waters, J. Phys. Oceanogr., 34, 3–22, doi:10.1175/1520-0485(2004)034<0003:tnpcow>2.0.co;2, 2004.

BGD
10, 11969–12008, 2013

Suggett, D. J., MacIntyre, H. L., and Geider, R. J.: Evaluation of biophysical and optical determinations of light absorption by photosystem II in phytoplankton, Limnol. Oceanogr.-Meth., 2, 316–332, 2004.
Suggett, D. J., Moore, C. M., Hickman, A. E., and Geider, R. J.: Interpretation of fast repetition rate (FRR) fluorescence: signatures of phytoplankton community structure versus physiological state, Mar. Ecol.-Prog. Ser., 376, 1–19, doi:10.3354/meps07830, 2009.
Sunda, W. G.: Feedback interactions between trace metal nutrients and phytoplankton in the ocean, Front. Microbiol., 3, 204, doi:10.3389/fmicb.2012.00204, 2012.
Thomson, R. E. and Fine, I. V.: Estimating mixed layer depth from oceanic profile data, J. Atmos. Ocean. Tech., 20, 319–329, doi:10.1175/1520-0426(2003)020<0319:emldfo>2.0.co;2, 2003.
Uitz, J., Claustre, H., Morel, A., and Hooker, S. B.: Vertical distribution of phytoplankton communities in open ocean: an assessment based on surface chlorophyll, J. Geophys. Res.-Oceans, 111, C08005, doi:10.1029/2005jc003207, 2006.
Vassiliev, I. R., Kolber, Z., Wyman, K. D., Mauzerall, D., Shukla, V. K., and Falkowski, P. G.: Effects of iron limitation on photosystem-II composition and light utilization in *Dunaliella-tertiolecta*, Plant Physiol., 109, 963–972, 1995.
Walker, N. D.: Satellite-observations of the Agulhas Current and episodic upwelling south of Africa, Deep-Sea Res. Pt. I, 33, 1083–1106, doi:10.1016/0198-0149(86)90032-4, 1986.
Woodward, E. M. S. and Rees, A. P.: Nutrient distributions in an anticyclonic eddy in the North East Atlantic Ocean, with reference to nanomolar ammonium concentrations, Deep-Sea Res. Pt. II, 48, 775–794, 2001.
Yentsch, C. S. and Phinney, D. A.: A bridge between ocean optics and marine ecology, Limnol. Oceanogr., 34, 1694–1705, 1989.
Zubkov, M. V., Fuchs, B. M., Tarran, G. A., Burkill, P. H., and Amann, R.: High rate of uptake of organic nitrogen compounds by Prochlorococcus cyanobacteria as a key to their dominance in oligotrophic oceanic waters, Appl. Environ. Microb., 69, 1299–1304, doi:10.1128/aem.69.2.1299-1304.2003, 2003.

BGD
10, 11969–12008, 2013

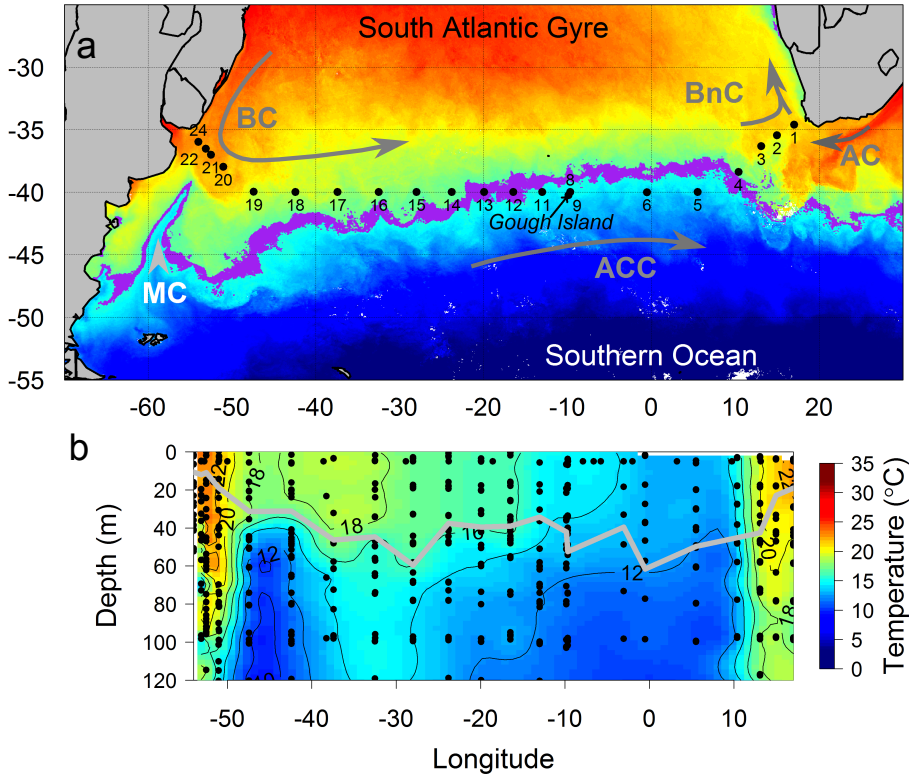

Fig. 1. Water temperature around the Atlantic SSTC. **(a)** MODIS monthly composite image of sea-surface temperature (SST) for January 2012. Dominant surface water masses and sampling stations are labelled (AC: Agulhas Current; ACC: Antarctic Circumpolar Current; BC: Brazil Current; BnC: Benguela Current; MC: Malvinas (Falklands) Current). Purple colouring represent SST = 16 °C (± 0.5 °C) and is shown as a practical definition of the SSTC location. Gough Island is located next to Station 9. **(b)** Cross-basin section of CTD water temperature. Grey line indicates the mixed layer depth (MLD).

BGD
10, 11969–12008, 2013

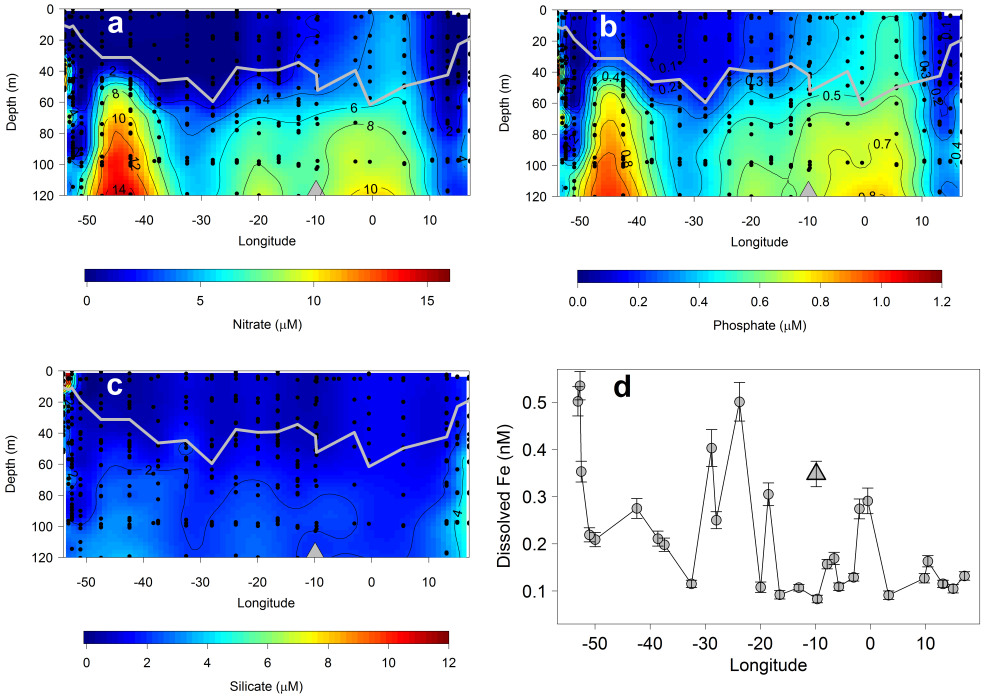

Fig. 2. Cross-basin section of macronutrient concentrations: **(a)** nitrate; **(b)** phosphate; **(c)** silicate. Grey lines indicate the MLD and grey triangles indicate the location of Gough Island. **(d)** Surface (~ 2–5 m) dissolved Fe concentrations. Error bars represent the standard deviation calculated as the accuracy of the spike ratio (~ 4 %) and the counting accuracy of the ICP-MS. The point labelled with a triangle represents the DFe concentration for Station 9 (next to Gough Island).

BGD
10, 11969–12008, 2013

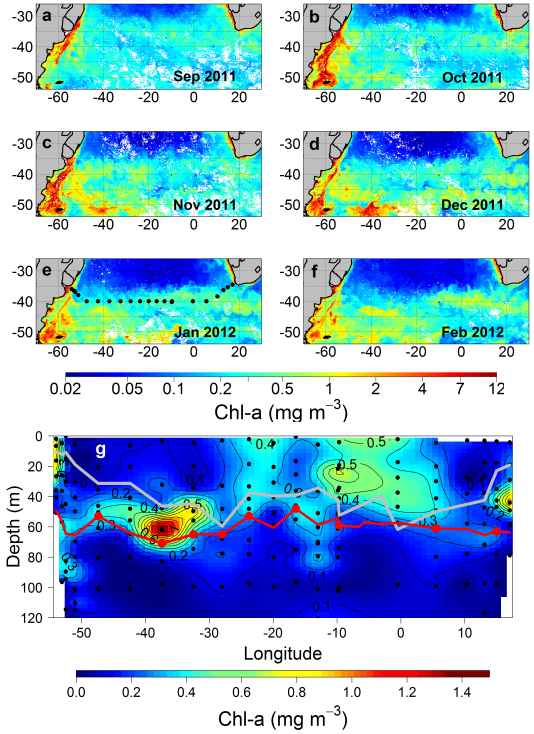

Fig. 3. MODIS monthly composite images **(a–f)** of chlorophyll *a* concentrations for September 2011–February 2012 around the Atlantic SSTC. Sampling locations are labelled for the January 2012 image which was the month of in situ sampling. **(g)** Cross-basin section of HPLC-derived chlorophyll *a* concentrations. Grey line is the MLD. The red line is the euphotic depth (z_{eu}) here defined as the 1 % light depth, with red dots indicating where direct PAR measurements were used to calculate the depth and remaining variability reflecting z_{eu} estimated using a derived chlorophyll-K_d relationship (K_d = 0.016 Chlorophyll *a* + 0.068).

BGD
10, 11969–12008, 2013

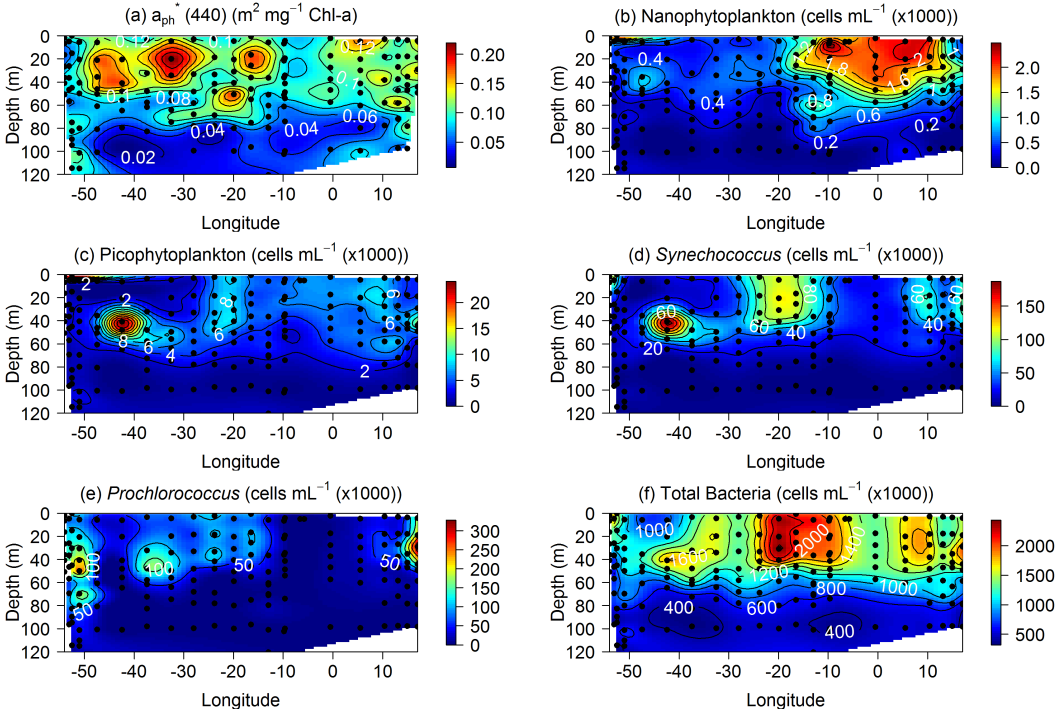

Fig. 4. Cross-basin (depth-longitude) sections of **(a)** specific phytoplankton absorption at 440 nm, and analytical flow cytometry counts of: **(b)** nanophytoplankton; **(c)** picophytoplankton; **(d)** *Synechococcus*; **(e)** *Prochlorococcus*; **(f)** total bacteria.

BGD
10, 11969–12008, 2013

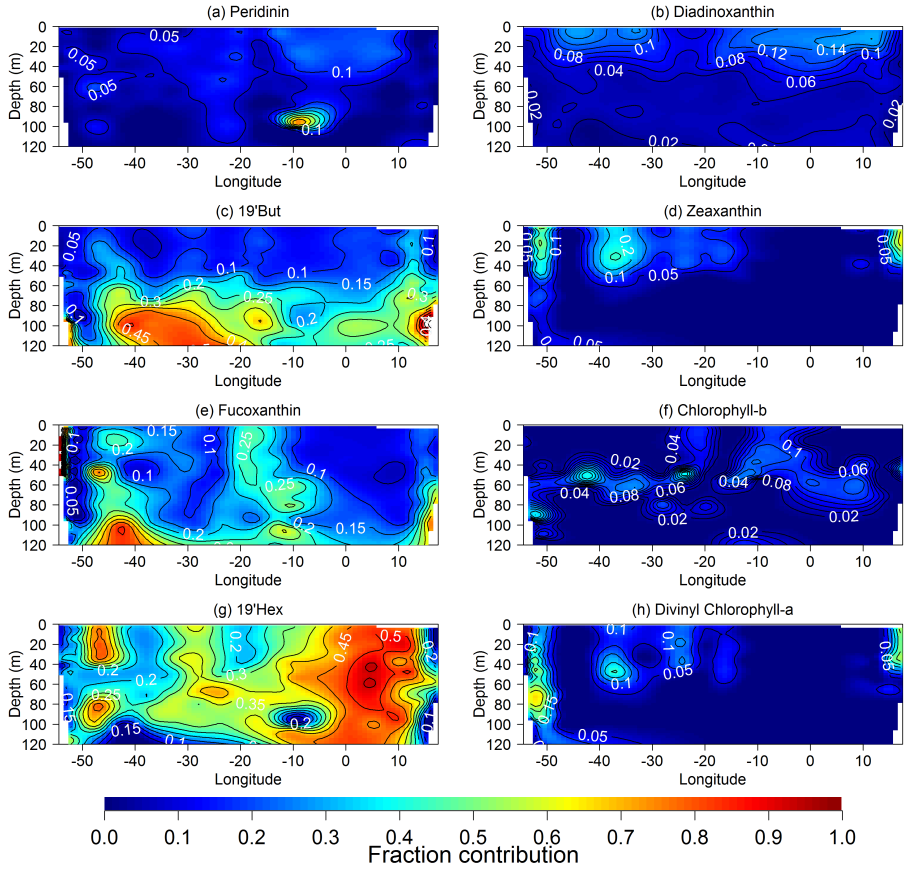

Fig. 5. Cross-basin (depth-longitude) sections of the contribution of major diagnostic pigments to total diagnostic pigments (19′Hex = 19′ hexanoyloxyfucoxanthin, 19′But = 19′ butanoyloxy-fucoxanthin).

BGD
10, 11969–12008, 2013

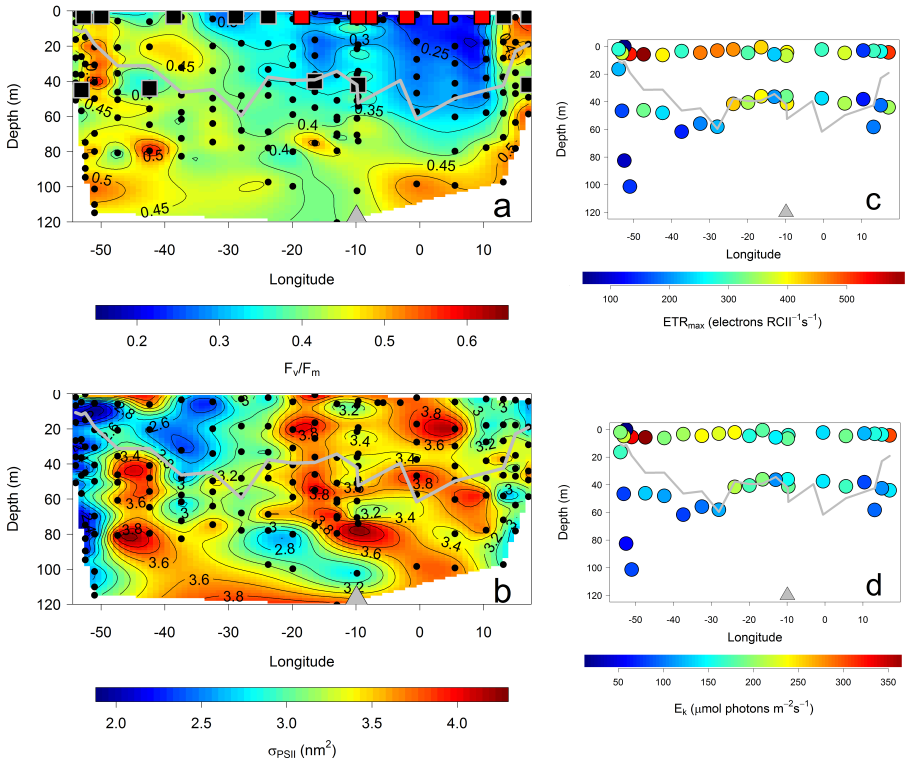

Fig. 6. Cross-basin sections of FRRf-derived photophysiological parameters: **(a)** F_v/F_m; **(b)** σ_{PSII}; **(c)** relative ETR$_{max}$; **(d)** E_k. Black and red squares in **(a)** indicate the location of Fe addition incubation experiments (black = no significant response from Fe amendment; red = statistically significant response). Grey lines indicate the MLD, grey triangles indicate the location of Gough Island.

BGD
10, 11969–12008, 2013

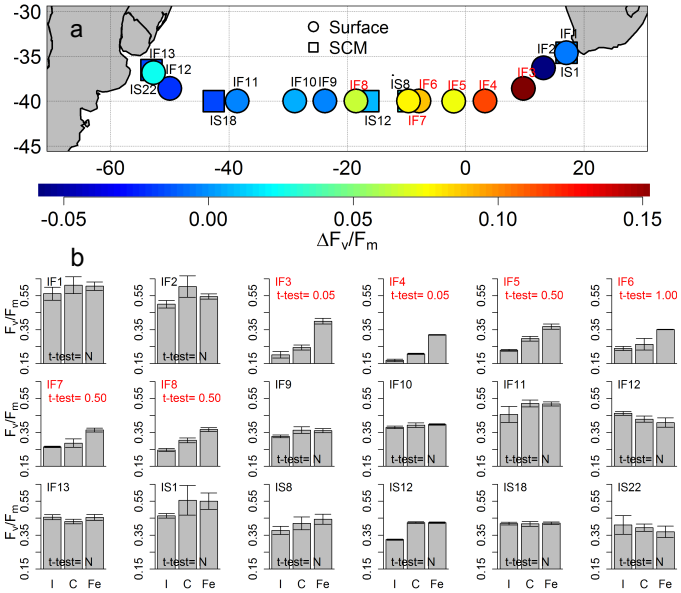

Fig. 7. Fe incubation locations and results. **(a)** Locations of experiments coloured according to $\Delta F_v/F_m$ values ($\Delta F_v/F_m = F_v/F_m$ Fe amended bottle – F_v/F_m control bottle). IF = Incubation Fish (indicating trace-metal-clean tow-fish water used for the experiment, highlighted on the map as a filled circle), IS = Incubation Station (indicating SCM trace-metal-clean water from the titanium CTD rosette was used, highlighted on the map as a filled square). Experiments with statistically significant responses (*t* test $p < 0.01$) are highlighted with red labels. **(b)** F_v/F_m for incubation experiments. I = Initial, C = Control (incubated for 24 h with no amendment), Fe = Fe spiked (incubated for 24 h after 2 nmol L^{-1} $FeCl_3$ addition). Bars = mean of three bottle replicates; error bars = standard deviation. Student's one tailed *t* test significance levels (%) are shown, with significant results labelled in red (N = no significant difference between control and Fe amended bottles).

BGD
10, 11969–12008, 2013

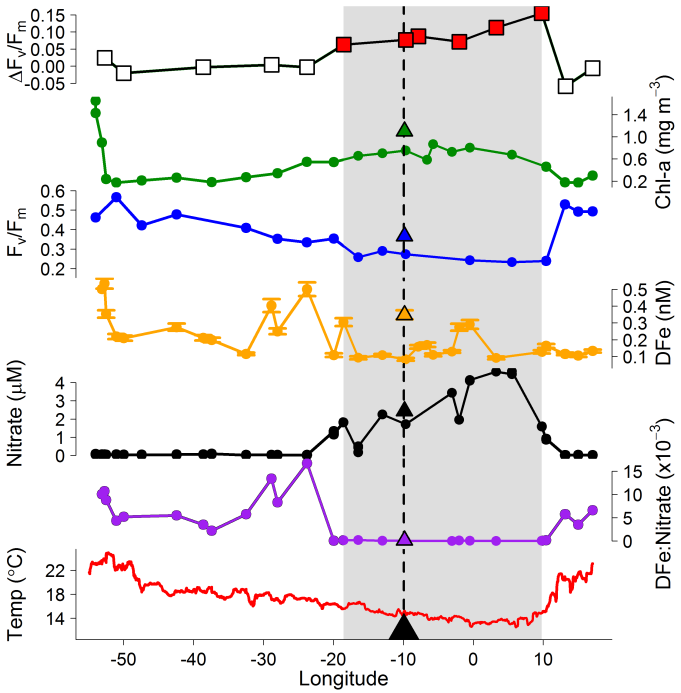

Fig. 8. Across-basin summary of: $\Delta F_v/F_m$ from Fe addition incubation experiments; chlorophyll *a*; F_v/F_m; nitrate; DFe; DFe : nitrate; ship's underway temperature. All measurements are from the surface (< 10 m depth) apart from F_v/F_m, shown for 20 m to reduce the influence of long-lived photodamage/PSII down-regulation on measurements. For $\Delta F_v/F_m$, red squares = statistically-significant response from Fe amended bottles. The grey shaded region highlights the Fe-limited zone as indicated by significant Fe amendment responses. Triangular symbols represent measurements from the station next to Gough Island, the location of which is highlighted by the large black triangle and dashed line.

BGD
10, 11969–12008, 2013